

Structural and Optical Properties of Polycrystalline ZnO Nanopowder Synthesized by Direct Precipitation Technique

Suresh Kumar^{1,2,*}, Divya Arora³, Anu Dhupar⁴, Vandana Sharma¹,
J.K. Sharma¹, S.K. Sharma⁵, Anurag Gaur⁶

¹ Department of Physics, Maharishi Markandeshwar (Deemed to be University), Mullana 133207, Haryana, India

² Department of Physics, Maharishi Markandeshwar University, Sadopur, Ambala 134007, Haryana, India

³ Kimberley the International School, Samanwa, Hangola, Panchkula 134204, Haryana, India

⁴ Department of Physics, Chandigarh University, Gharoun, Mohali 140413, Punjab, India

⁵ School of ICT, Gautam Buddha University, Greater Noida 201308, Uttar Pradesh, India

⁶ Department of Physics, National Institute of Technology, Kurukshetra 136119, Haryana India

(Received 27 April 2020; revised manuscript received 15 August 2020; published online 25 August 2020)

ZnO nanopowder has been synthesized by direct precipitation technique at ambient conditions using zinc chloride and sodium hydroxide as primary precursors. The structural, morphological and optical properties of ZnO nanopowder have been examined by X-ray diffraction (XRD), field effect scanning electron microscopy (FE-SEM), energy dispersive spectroscopy (EDX), FT-IR, and UV-Visible diffuse reflectance spectroscopy. The XRD analysis shows that ZnO nanopowder is polycrystalline in nature and has a wurtzite structure. The synthesized nanopowder possesses single-phase crystallites which are highly oriented in (101) reflection plane. EDX analysis confirms the presence of lone Zn and O content in the nanopowder which is almost stoichiometric in the proportion. The surface morphology of ZnO nanopowder has been analyzed by FE-SEM and it was found that the excessive surface energy of the nanoparticles is responsible for the random orientation and agglomeration. The interaction of different functional groups during the synthesis has been identified from the FT-IR spectrum. The presence of distinct absorption peaks and bands at respected wavenumbers confirms the successful formation of ZnO from the different chemicals used in the synthesis. The optical bandgap has been estimated from the Kubelka-Munk plot by extrapolating the linear portion of the curve on the energy axis. The existence of the particles in the nanorange and a high optical bandgap value support the quantum confinement effect in ZnO nanopowder.

Keywords: ZnO, Precipitation technique, XRD, FE-SEM, FT-IR, Optical properties.

DOI: [10.21272/jnep.12\(4\).04027](https://doi.org/10.21272/jnep.12(4).04027)

PACS numbers: 78.66.Hf, 78.67.Bf, 61.05.cp, 82.80.Gk

1. INTRODUCTION

Metal oxides are excellent multifunctional semiconductors which have demonstrated excellent applications in different domains of research and industry for many decades. The future prospective of metal oxides brings them to the exciting field of nanotechnology where they are experiencing excellent and diverse applications [1-4]. Zinc oxide (ZnO) belongs to II-VI family of periodic table of elements. It is a wide bandgap oxide semiconductor having a direct bandgap value between 3.2 to 3.4 eV in the bulk form [5]. It exists in three crystal structures which are wurtzite, zinblende, and rocksalt [3]. ZnO is nontoxic, biocompatible, widespread in nature and has large exciton binding energy, transparent conductivity, exhibiting near UV emission, high oxidation capability, high chemical and mechanical stability [3, 4]. It has been widely explored by researchers because of its potential applications in the numerous fields including short wavelength range electronics, piezoelectric transducers, UV-Visible display devices, space detectors, surface acoustic devices, solar cells, transparent electrodes, chemical and gas sensors, photocatalysis, spintronics and so on [6, 7]. It is frequently used in biomedical applications including personal care products, such as cosmetics, deodorants and sunscreens due to its strong antibacterial, antimicrobial and UV-blocking properties [8].

Many simple and cost-effective as well as complicat-

ed and expensive techniques have been employed for the synthesis of ZnO nanoparticles which include hydrothermal, soft chemical synthesis, precipitation, sol-gel, microwave-assisted methods, pyrolysis, gas condensation, laser ablation, and so on [6-8]. However, liquid phase direct precipitation technique has attracted in recent years because of its simplicity, low cost, and rapid synthesis of ZnO nanoparticles [9, 10]. Additionally, this technique is capable of reproducing ZnO nanoparticles with the same parameters and allows easy control of the size, structure, morphology and other properties of the final product [9]. Therefore, this work is dedicated to synthesize ZnO nanopowder using liquid phase direct precipitation technique and characterize them for different properties using X-ray diffraction (XRD), field effect scanning electron microscopy (FE-SEM), Fourier transform infrared spectroscopy (FT-IR) and UV-Visible diffuse reflectance spectroscopy.

2. EXPERIMENTAL DETAILS

The analytical reagent (AR) grade chemicals with 99.9 % purity were used in the synthesis process and are obtained from Merck (India). ZnO nanopowder was synthesized by direct precipitation technique using aqueous ammonia hydroxide (NaOH: 0.5 M and 20 ml) solution mixed slowly with zinc chloride anhydrous (ZnCl₂.H₂O: 0.05 M and 20 ml) solution under vigorous stirring using

* sureshlakhanpal@gmail.com

a hot plate magnetic stirrer. Ammonia solution (NH₄OH: 25 % and 5 ml) was used to control the pH of the final solution. The whole experimentation was performed at room temperature under ambient conditions, at pH to 10.5 and a continuous stirring rate of 300 rpm. The final solution was stirred continuously for 1 h and the milky white precipitate was obtained as a result of precipitation. These precipitates were collected by centrifugation at 8000 rpm for 10 min (Remi, India) and washed consecutively with acetone and double-distilled water. Finally, the obtained powder sample was calcined at 500 °C in an air atmosphere for 3 h in a muffle furnace.

2.1 Characterization of ZnO Nanopowder

Different techniques were used to characterize the synthesized ZnO nanopowder. Crystal structure and structural parameters were characterized using XRD. The XRD pattern was obtained using XRD (PANalytical X'PERT-PRO diffractometer) with CuK α radiation ($\lambda = 1.5406 \text{ \AA}$) of 40 kV and 30 mA with a step size of 0.017° and in a scanning range, $2\theta = 20^\circ$ to 80° . The structural morphological features, especially the shape of ZnO nanopowder, were determined using FE-SEM (JEOL JSM-6100) where the sample was prepared in ethanol solution and sonicated with ultrasonic cleaner for 30 min. Elemental composition was quantified by energy dispersive X-ray (EDX) analyzer, model Bruker Quantax 200 attached with FE-SEM. FT-IR spectroscopy was used to identify the surface functional group that was present in the nanopowder using FT-IT spectrometer (Perkin Elmer 1600) and the sample was prepared using KBr pellet technique. Ultraviolet-visible (UV-Vis) diffuse reflectance spectroscopy was performed for the optical analysis using UV-Vis spectrometer (SCHIMAZDU 2600) for the wavelength range of 200 nm to 800 nm in the air at room temperature.

3. RESULTS AND DISCUSSION

3.1 XRD Analysis

The XRD study has been performed to analyze the structure and purity of ZnO nanopowder. XRD spectrum for the as-synthesized ZnO nanopowder is shown in Fig. 1.

The XRD analysis revealed that ZnO nanopowder is crystallized in wurtzite (hexagonal) structure which belongs to the space group P63mc (JCPDS card number 036-1451). The multiple diffraction peaks existing in XRD spectra at different 2θ values are indexed to different Miller indices (hkl) which are listed in Table 1.

The intensity of these diffraction peaks has been found maximum at $2\theta/(hkl) = 36.27^\circ/(101)$ which means that the majority of the particles in the nanopowder sample are oriented in (101) direction. It has been analyzed that 2θ positions, intensities, d -spacing and (hkl) values of the diffraction peaks are consistent with the standard values (JCPDS data card 036-1451) as well as with the previous reports [7, 11, 12]. Moreover, it has been analyzed that ZnO nanopowder possesses single-phase crystallites without any impurity and good crystallinity. Similar results for ZnO phase formation using different methods have been reported earlier in literature [6, 7, 11]. This means that the direct precipitation technique is capable of producing pure phase of ZnO nanoparticles in a simple and cost-effective way.

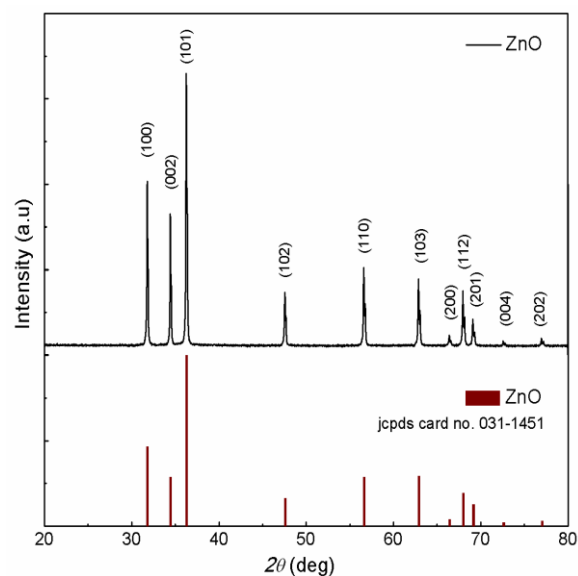


Fig. 1 – The XRD spectrum as observed (top) and standard (bottom) for ZnO nanopowder

Table 1 – Different structural parameters (observed and standard values) for ZnO nanopowder estimated from XRD spectrum

Observed values for the structural parameter			Standard value from JCPDS card no. 036-1451			Miller indices (hkl)	FWHM (deg)	Particle size (nm)	Micro strain ($\times 10^{-3}$)	Dislocation density (line/m^{-2})
2θ (deg.)	Intensity (%)	d -spacing (\AA)	2θ (deg.)	Intensity (%)	d -spacing (\AA)					
31.79	61.90	2.813	31.80	46.51	2.8140	(100)	0.1504	57.36	2.30	3.04×10^{14}
34.43	50.60	2.603	34.45	28.63	2.6034	(002)	0.1504	57.76	2.12	3.00×10^{14}
36.27	100.00	2.475	36.29	100.00	2.4755	(101)	0.1671	52.24	2.23	3.66×10^{14}
47.55	22.60	1.911	47.58	16.31	1.9111	(102)	0.2172	41.74	2.15	5.74×10^{14}
56.70	31.30	1.625	56.65	28.85	1.6248	(110)	0.1169	80.65	9.47	1.54×10^{14}
62.87	27.20	1.477	62.92	29.33	1.4771	(103)	0.1336	72.79	9.54	1.89×10^{14}
66.46	07.60	1.406	66.46	4.02	1.4068	(200)
67.97	23.50	1.378	68.02	19.35	1.3783	(112)	0.1336	74.90	8.65	1.78×10^{14}
69.11	13.00	1.358	69.17	12.68	1.3581	(201)	0.3342	30.15	2.12	11.0×10^{14}
72.55	05.40	1.302	72.63	2.22	1.3017	(004)
77.13	06.30	1.238	77.05	3.16	1.2377	(202)

The average particle size (D_a) of the nanoparticles is estimated after background correction from X-ray line broadening of the diffraction peaks using Debye-Scherrer formula [12]

$$D_a = \frac{0.94\lambda}{\beta_{2\theta} \cos \theta_{hkl}},$$

where 0.94 is the Scherrer constant, λ is the wavelength of X-rays, θ is the Bragg diffraction angle and β is the full width at half maximum (FWHM) of diffraction peak. The different structural parameters [11, 12] such as d -spacing, microstrain, dislocation density, lattice constants of ZnO nanopowder are calculated and represented in Table 1 and Table 2. The average values of the particle size, microstrain, and dislocation density are 58.5 nm, 1.71×10^{-3} and 3.96×10^{14} line/m² respectively. Some variations in lattice parameters may be associated with the size of particles in the nanorange and the presence of oxygen vacancies.

3.2 FE-SEM and EDX Analysis

The FE-SEM micrograph of the prepared ZnO nanopowder is shown in Fig. 2a. The randomly oriented and elongated shaped nanoparticles in huge agglomeration are observed in the micrograph. The excessive surface energy on the surface of the nanoparticles may be responsible for agglomeration.

EDX spectrum (Fig. 2b) confirms that synthesized ZnO nanopowder is of high purity because only Zn and O content is detected in it. In addition, the as-prepared nanopowder is almost stoichiometric (slightly oxygen-deficient) where Zn/S = 1.06 at. %. These oxygen deficiencies may lead to change in lattice parameters as expected in XRD analysis. No other elements are traced out which show that this synthesis technique helps to prepare pure and stoichiometric ZnO nanopowder.

3.3 FT-IR Analysis

FT-IR spectrum of ZnO nanopowder (Fig. 3) represents many absorption peaks and bands corresponding to different functional groups at 536.9, 698.5, 788.5, 875.2, 984.9, 1131.6, 1383.7, 1427.0, 1631.8, 2068.8 and 3424.0 cm⁻¹. The broad absorption band at 3424 cm⁻¹ is attributed to O–H stretch of adsorbed water-bound at oxides surface. A medium peak at ~ 1631 cm⁻¹ may also be related to O–H bending vibrations of water molecules trapped in these oxides during their formation [13]. The medium band at about 2068.8 cm⁻¹ is attributed to N–H stretching vibrations [14]. These peaks arise due to the use of ammonia in the synthesis process. The weak peaks in the range 1300 to 1450 cm⁻¹ and ~ 1131 cm⁻¹ correspond to the asymmetric and symmetric C=O and C–O stretching bonds, respectively [10]. The weak absorption

peaks at 875 cm⁻¹ and 984 cm⁻¹ belong to O–H out of plane bending vibration of H₂O molecules [10]. The metal-oxygen stretching frequencies appear in the lower wavenumber range. The wavenumbers of 536.9, 698.5 and 788.5 cm⁻¹ are assigned to Zn–O bond vibrations similar to another report [15].

The presence of these functional groups confirms the successful formation of ZnO from the different precursors used in the synthesis. The FT-IR analysis has also validated the results obtained from XRD analysis.

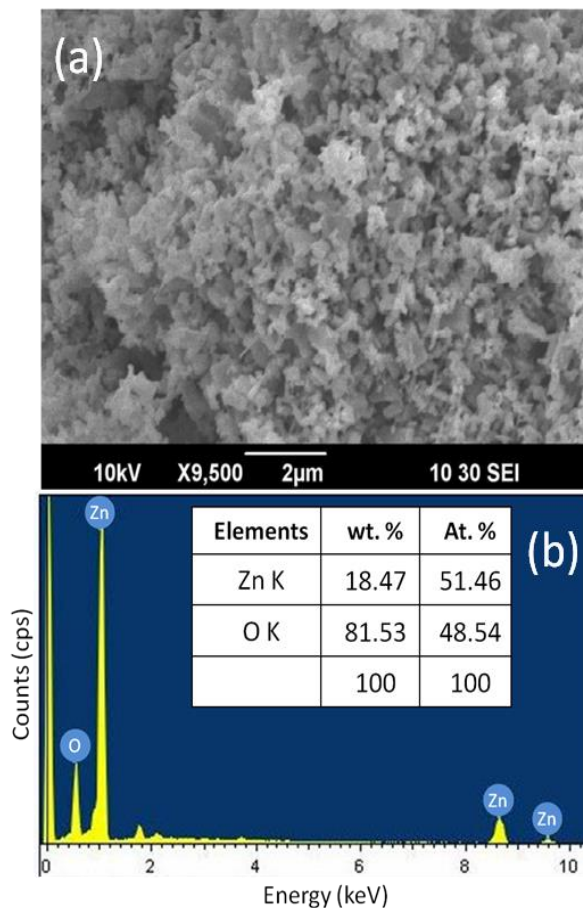


Fig. 2 – (a) FE-SEM micrograph and (b) EDX spectrum with tabulated elemental quantification of ZnO nanopowder

3.4 Optical Analysis

The optical properties of ZnO nanopowder have been analyzed by UV-Vis diffuse reflectance spectroscopy. The absorption edge is a characteristic of the optical parameter and related to the intrinsic bandgap of the semiconductor materials. From the absorption spectra (Fig. 4a), the absorption edge of ZnO nanopowder has been observed at ~ 358 nm and this value is in good agreement with the reported values [16].

Table 2 – Different structural parameters (observed and standard values) for ZnO nanopowder estimated from XRD spectrum

	Lattice parameters				Absorption edge (nm)	Optical bandgap (eV)
	a (Å)	c (Å)	c/a ratio	Unit cell volume (Å ³)		
ZnO nanopowder	3.248	5.205	1.603	47.55	358	3.46
JCPDS card no. 036-1451	3.249	5.206	1.602	47.63	400-375	3.1-3.3

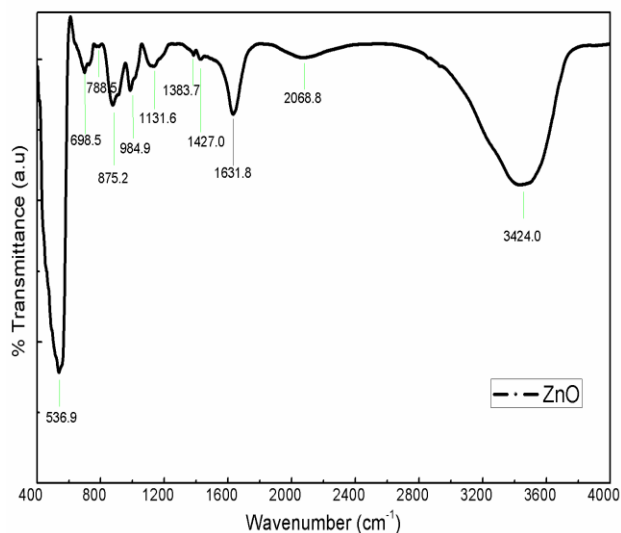


Fig. 3 – FT-IR spectrum of ZnO nanopowder

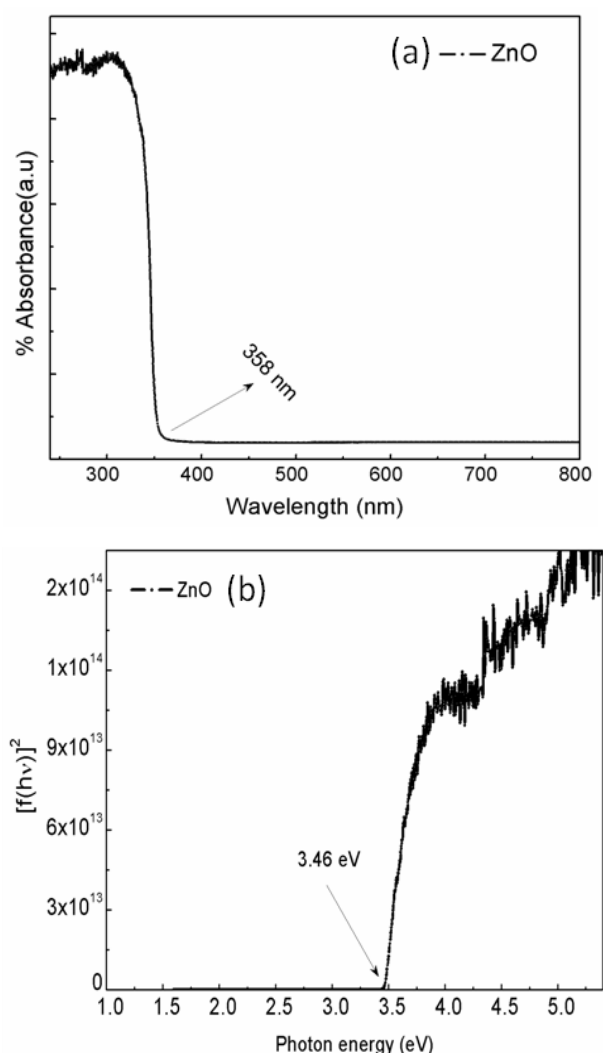


Fig. 4 – (a) UV-Vis absorption spectrum of ZnO nanopowder; (b) plot of Kubelka-Munk function versus the photon energy of absorbed light for ZnO nanopowder

The optical bandgap (E_g) and the nature of the transition in ZnO sample have been determined by the Kubelka-Munk relationship [17] as

$$[F(R)h\nu]^2 = B(h\nu - E_g),$$

where $F(R) = (1 - R)^2/2R$ is the Kubelka-Munk function, R is the percentage of reflected light, $h\nu$ is the incident photon energy, B is a constant depending on the transition probability. The plot of $[F(h\nu)]^2$ as a function of the photon energy ($h\nu$) of the incident radiation is shown in Fig. 4b. It is found that the nature of the plot is nonlinear indicating the absence of indirect transition.

The value of E_g has been evaluated from the intercept of the extrapolated linear part of the curve on the energy axis and found to be 3.46 eV. This value is slightly higher than the range of values from 3.1 eV to 3.3 eV for bulk ZnO as reported in literature [11, 12, 5], but in good agreement with the values for ZnO nanoparticles [16]. This high value of the optical bandgap could be attributed to the presence of nanoparticles in the ZnO sample and also to the existence of the quantum confinement effect.

4. CONCLUSIONS

ZnO nanopowder has been synthesized by direct precipitation technique at ambient conditions. The properties of ZnO nanopowder have been explored by XRD, FE-SEM, EDX, FT-IR, and UV-Vis spectroscopy. The XRD analysis revealed that ZnO nanopowder is polycrystalline in nature and has a wurtzite structure. The average particle size of ZnO nanoparticles has been estimated to 58 nm by Debye-Scherrer formula. The randomly oriented, highly agglomerated and elongated shaped nanoparticles have been observed from the FE-SEM. EDX analysis confirms the synthesis of pure and almost stoichiometric (Zn/S = 1.06 at. %) ZnO nanopowder. Moreover, the existence of a few oxygen deficiencies and the nanosize of the particles leads to the variation in the lattice parameters. The characteristic peak region for Zn–O stretching has been identified between the wavenumbers 500 cm^{-1} to 800 cm^{-1} . The presence of distinct absorption peaks and bands authenticates the successful synthesis of ZnO nanopowder from the employed chemicals. The optical bandgap is calculated to be 3.46 eV which is higher than the value of bulk ZnO particles. This high value of the optical bandgap may be due to the presence of nanoparticles and the associated quantum confinement effect. The synthesized ZnO nanopowder can be used in different applications such as display material for electronic items, biological agents, photocatalysis, energy harvesting and so forth.

ACKNOWLEDGEMENTS

The authors acknowledge SAIF Chandigarh for XRD, FE-SEM, EDX and FT-IR facilities, and Chandigarh University for UV-Vis-NIR diffuse reflectance spectroscopy.

REFERENCES

1. A.V. Nikam, B.L.V. Prasad, A.A. Kulkarni, *Cryst. Eng. Comm.* **20**, 5091 (2018).
2. M.S. Chavali, M.P. Nikolova, *SN Appl. Sci.* **1**, 607 (2019).
3. G.C. Yi, C. Wang, W. Park, *Semicond. Sci. Technol.* **20**, S22 (2005).
4. T. Chitradevi, A.J. Lenus, N.V. Jaya, *Mater. Res. Express* **7**, 015011 (2020).
5. V. Srikant, D.R. Clarke, *J. Appl. Phys.* **83**, 5447 (1998).
6. M.A. Borysiewicz, *Crystals* **9**, 505 (2019).
7. J. Guo, C. Peng, *Ceram. Int.* **41**, 2180 (2015).
8. J. Jiang, J. Pi, J. Cai, *Hindawi Bioinorg. Chem. Appl.* **2018**, 1062562 (2018).
9. A.K. Radzimska, T. Jesionowski, *Materials* **7**, 2833 (2014).
10. S. Kumar, J.K. Sharma, *Mater. Sci. Poland* **34**, 368 (2016).
11. M. Kahouli, A. Barhoumi, A. Bouzid, A. Al-Hajry, S. Guermazi, *Superlatt. Microstruct.* **85**, 7 (2015).
12. P.G. Devi, A.S. Velu, *Synthesis, J. Theor. Appl. Phys.* **10**, 233 (2016).
13. Ö. Acarbaş, E. Suvac, A. Doğan, *Ceram. Int.* **33**, 537 (2007).
14. R.K. Sharma, R. Ghose, *Ceram. Int.* **40**, 10919 (2014).
15. N.F. Djaja, D.A. Montja, R. Saleh, *Adv. Mater. Phys. Chem.* **3**, 29130 (2013).
16. S. Talam, S.R. Karumuri, N. Gunnam, *ISRN Nanotech.* **2012**, 372505 (2012).
17. A. Dhupar, S. Kumar, V. Sharma, J.K. Sharma, *Mater. Sci. Poland* **37**, 230 (2019).

Структурні та оптичні властивості полікристалічного нанопорошку ZnO, синтезованого методом прямого осадження

Suresh Kumar^{1,2}, Divya Arora³, Anu Dhupar⁴, Vandana Sharma¹,
J.K. Sharma¹, S.K. Sharma⁵, Anurag Gaur⁶

¹ Department of Physics, Maharishi Markandeshwar (Deemed to be University), Mullana 133207, Haryana, India

² Department of Physics, Maharishi Markandeshwar University, Sadopur, Ambala 134007, Haryana, India

³ Kimberley the International School, Samanwa, Hangola, Panchkula 134204, Haryana, India

⁴ Department of Physics, Chandigarh University, Gharraun, Mohali 140413, Punjab, India

⁵ School of ICT, Gautam Buddha University, Greater Noida 201308, Uttar Pradesh, India

⁶ Department of Physics, National Institute of Technology, Kurukshetra 136119, Haryana India

Нанопорошок ZnO був синтезований методом прямого осадження в умовах навколишнього середовища, використовуючи хлорид цинку та гідроксид натрію як первинні прекурсори. Структурні, морфологічні та оптичні властивості нанопорошку ZnO були досліджені за допомогою рентгенівської дифракції (XRD), польової скануючої електронної мікроскопії (FE-SEM), енергетично-дисперсійної спектроскопії (EDX), FT-IR, та UV-Visible спектроскопії дифузного відбиття. Аналіз XRD показує, що нанопорошок ZnO має полікристалічну природу та структуру вюрциту. Синтезований нанопорошок складається з однофазних кристалітів, високоорієнтованих у площині відбиття (101). Аналіз EDX підтверджує наявність у нанопорошку вмісту окремих Zn та O, склад яких є майже стехіометричним у пропорції. Морфологія поверхні нанопорошку ZnO була проаналізована методом FE-SEM і було встановлено, що надмірна поверхнева енергія наночастинок відповідає за випадкову орієнтацію та агрегацію. Взаємодія різних функціональних груп під час синтезу була визначена з спектру FT-IR. Наявність чітких піків поглинання та смуг для стандартних хвильових чисел підтверджує успішне утворення ZnO з різних хімічних речовин, що використовуються в синтезі. Ширина оптичної забороненої зони була оцінена за графіком Кубелка-Манка шляхом екстраполяції лінійної частини кривої на вісь енергій. Наявність частинок у нанодіапазоні та високе значення ширини оптичної забороненої зони підтримують ефект квантового утримання в нанопорошку ZnO.

Ключові слова: ZnO, Техніка осадження, XRD, FE-SEM, FT-IR, Оптичні властивості.